PHYSICAL REVIEW B

CONDENSED MATTER

THIRD SERIES, VOLUME 49, NUMBER 18 1 MAY 1994-II

Line-shape description for Mössbauer conversion-electron and transmission geometries

R. A. Wagoner and J. G. Mullen

Physics Department, Purdue University, West Lafayette, Indiana 47907

(Received 8 September 1992; revised manuscript received 13 December 1993)

We derive an approximate integral line-shape expression for conversion-electron Mössbauer spectroscopy and for the single-foil microfoil internal conversion-electron detector, which includes asymmetry (interference) effects, finite thickness of foils, and the presence of resonance absorption in the source material. We then give an analytical expansion that is equivalent to this integral expression and which is usable for computer least-squares fitting. We also give the exact integral line-shape expression for Mössbauer transmission experiments using finite thickness absorbers, which includes asymmetry effects and source resonance self-absorption, along with its convergent analytic expansion. The inclusion of hyperfine interactions and the practical approach to using the line-shape analysis to minimize the correlation of parameters is discussed.

I. INTRODUCTION

The line shape found using conversion-electron Mössbauer spectroscopy (CEMS) represents the intensity of electrons emitted from the face of a resonantly absorbing material as a function of a Doppler velocity (of source or absorber). In general only the backscattered electrons are measured, and the line shape in this case is described by $C_-(x)$, where x represents the Doppler velocity and $C_-(x)$ the number of counts associated with x (counts per channel).

In standard conversion spectroscopy thick foils are used to achieve sufficient γ-ray absorption. But these thicker foils result in loss of electron detection since electrons emitted deep within the foil tend to be reabsorbed, or their energy greatly diminished, before they can reach the surface. An alternate method is to use a microfoil internal conversion-electron (MICE) detector.[1,2] The MICE detector, shown in Fig. 1, uses multiple very thin foils placed in tandem in the γ-ray beam, with collection wires placed between the foils, which allows the emitted electrons to escape the foil while retaining appreciable absorption, since the multiple foils can have an appreciable total thickness. In the case of a single-foil MICE detector, the line shape of the backscattered electrons, $C_-(x)$, as well as that of the forward scattered electrons, $C_+(x)$, can be measured. As mentioned in Ref. 1, the MICE detector also offers significantly increased percent effect for certain favorable cases over that attained by transmission Mössbauer experiments.

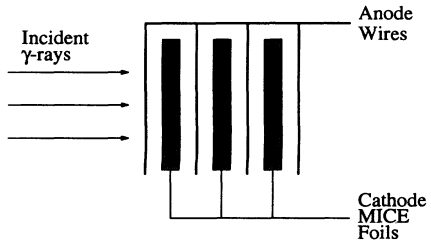

FIG. 1. Geometry of a MICE detector.

In both conversion and transmission experiments the use of incorrect line-shape analysis, such as Lorentzians which fail to correctly take into account finite absorber thickness, results in an incorrect determination of line-shape parameters. This includes inaccuracies in commonly measured parameters such as line width, as well as the Mössbauer asymmetry parameter, β,[3-6] which arises from interference effects between resonant nuclear and nonresonant inner shell electron processes. Another source of error is due to the presence of significant source resonance self-absorption (SRSA), which may affect the returned best-fit parameters adversely if not accounted for correctly. Our line-shape expression for conversion and single-foil MICE detectors is an approximation which includes SRSA and the effect of finite absorber (electron source) thickness. We also give the theoretical expression, including SRSA, for finite thickness absorber transmission experiments. The transmission case was originally worked out in Ref. 7, but that presentation has since been found to contain an error when SRSA is present. This error was not in the functional form, but in some of the constants that appear in the final expression. We accordingly give the corrected expression here. Since the mathematical details involved in solving for the integrals that appear in both the transmission and conversion cases are rather involved, and since they have been well explained in Ref. 7, we have not repeated them here. Both the conversion and transmission line shapes below

are for single line source and absorber systems, although the integral forms can be modified to include hyperfine interactions as we discuss in Sec. V.

II. CONVERSION LINE SHAPE

The distribution of resonant γ rays emitted from a source when SRSA is present is given by[7]

$$w_s(x')=C_s\frac{1-e^{-t_s(x')}}{t_s(x')[1+4x'^2]}\ , \tag{1}$$

where $x'=(E-E_o)/\Gamma$, E the γ-ray energy and E_o the transition energy as measured in the rest frame of the lab, Γ is the Heisenberg level width, $\hbar/\tau$, and

$$t_s(x')=\frac{t_{\rm rs}(1-4\beta x')}{1+4x'^2}+t_{\rm ns}\ , \tag{2}$$

where the source Mössbauer (resonant) thickness number is given by

$$t_{rs}=f_{\rm so}\sigma_o n_s a_s\ , \tag{3}$$

and $f_{\rm so}$ is the source recoilless fraction, n_s is the total mass per area of all types of atoms in the source material, a_s is the fraction of n_s that are of the Mössbauer type, and σ_o is the maximum resonant γ-ray-absorption cross section. The total nonresonant attenuation thickness number t_{ns} is given by $\sigma_{\rm ns}n_s$, where $\sigma_{\rm ns}$ is the nonresonant absorption cross section for the source material. We solve for C_s by choosing a normalization in which $w_s(y)$ integrated over all energy space is equal to the intensity of the resonant γ rays per unit energy (i.e., per channel) in the beam incident on the absorber, given by f_sC_o, where C_o is the total counts of γ rays (resonant and nonresonant) per channel in the incident beam, and f_s is that fraction which are resonant. From this we have

$$\int_{-\infty}^{\infty}w_s(y)dy=\frac{C_s(1-e^{-t_{\rm ns}})\pi\rho}{2t_{\rm ns}}\equiv f_sC_o\ , \tag{4}$$

from which

$$C_s=\frac{2t_{\rm ns}f_sC_o}{(1-\exp[-t_{\rm ns}])\pi\rho}\ , \tag{5}$$

where

$$\rho=\sum_{k=0}^{\infty}\frac{(2k)!\tau_k t_{rs}^k}{4^k(k!)^2}\ , \tag{6}$$

$$\tau_k=\frac{t_{\rm ns}(-1)^k}{(1-e^{-t_{\rm ns}})k!}\sum_{n=0}^{\infty}\frac{(-t_{\rm ns})^n}{n!(k+n+1)}\ . \tag{7}$$

The fraction f_s is less than the recoilless fraction of resonant γ rays, $f_{\rm so}$, produced in the source, since some γ rays are resonantly absorbed (SRSA) before they can exit the source. The two fractions are related by

$$f_s=\frac{\rho f_{\rm so}}{1-f_{\rm so}+\rho f_{\rm so}}\ . \tag{8}$$

The expression given in Eq. (8) differs from our earlier work[7] [Eq. (29)], by the factor shown in the denominator of Eq. (8). The two expressions are the same in the limit where t_{rs} is small, a condition that usually holds in good line-shape experiments, where there is little source resonance self-absorption.

The source is Doppler shifted relative to the conversion detector at a velocity v, the γ-ray distribution incident on the conversion detector is $w_s(X)$, where $X=x'-x$, $x=(E_o-E_r)/\Gamma$, and E_r represents the difference between the transition energy of the source Mössbauer effect (ME) nuclei and the absorber ME nuclei in the conversion detector. A schematic of the conversion γ-ray absorber and electron source is shown in Fig. 2, which we assume has a total mass per area of all types of atoms given by n_a, of which a fraction a_a are Mössbauer absorbing atoms. The resonant γ-ray intensity reaching the slice dn, is given by

$$I(x,x')=w_s(X)\exp[-(\sigma_{\rm ra}(x')+\sigma_{\rm na})n]\ ,$$

where the resonant absorption cross section with interference is

$$\sigma_{\rm ra}(x')=\frac{t}{n_a}\mathcal{L}(2x')\ , \tag{9}$$

and the Mössbauer thickness number for the entire width is

$$t=f_a\sigma_o a_a n_a\ , \tag{10}$$

with f_a the recoilless fraction of the absorber ME nuclei. The resonance behavior of the γ-ray cross section, including interference effects, is given by the term

$$\mathcal{L}(x')=(1-2\beta x')/(1+x'^2)\ . \tag{11}$$

The nonresonant γ-ray absorption cross section for the absorber material is given by $\sigma_{\rm na}$, where the nonresonant thickness number for the entire width is $t_{\rm na}=\sigma_{\rm na}n_a$.

We consider the electrons emitted (at all angles) in the forward (+) direction, that is, the face the γ-ray beam

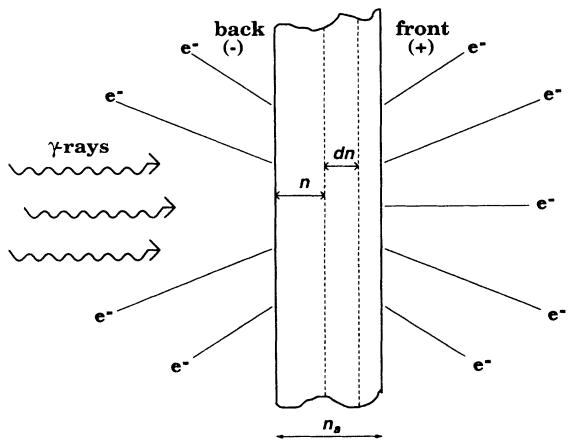

FIG. 2. Diagram of an absorber used in conversion spectroscopy.

exits (see Fig. 2). The number of both internal conversion and photoelectrons emitted in the forward direction from the slice dn is given by $I(x,x')[\sigma_{c+}(x')+\sigma_{p+}]dn$, where $\sigma_{c+}(x')$ is the cross section for conversion electrons to be scattered in the forward direction, and σ_{p+} is the similar cross section for photoelectric emission. We can write these scattering cross sections in terms of t and $t_{\rm na}$ by assuming that the photoelectric scattering is proportional to the nonresonant absorption, and that internal conversion electron emission is proportional to resonant absorption, so that

$$\sigma_{c+}(x')=r_{c+}\sigma_{\rm ra}(x')=\frac{r_{c+}t\mathcal{L}(2x')}{n_a}\ ,$$
$$\sigma_{p+}=r_{p+}\sigma_{\rm na}=\frac{r_{p+}t_{\rm na}}{n_a}\ , \tag{12}$$

where r_{p+} and r_{c+} are the fractions relating the scattering to the corresponding absorption cross sections. These scattered electrons must then pass through (n_a-n) material before they can emerge from the forward face and contribute to the measured signal. The absorption of charged particles which undergo multiple scattering is rather complex, but we assume that the attenuation of these electrons, totaled over the whole forward hemisphere, is approximately exponential,[8,9] so that the attenuation is given by $\exp[-t_e(n_a-n)/n_a]$, where t_e is the thickness number for electron absorption (averaged over all forward angles) for the entire width of the absorbing material (corresponding to n_a). The probability for electron emission from the forward face due to resonant γ rays corresponding to Doppler shift x, is then

$$P_+(x,x')=\frac{w_s(X)[r_{c+}t\mathcal{L}(2x')+r_{p+}t_{\rm na}]e^{-t_e}}{n_a}\times\int_o^{n_a}dn\,\exp[-(t\mathcal{L}(2x')+t_{\rm na}-t_e)n/n_a]\ . \tag{13}$$

This expression can be easily integrated, and it and an expression obtained in a similar manner for electrons ejected from the backward $(-)$ direction, and the two line-shape expressions written as a single mathematical equation. The total signal (electrons counted) due to resonant γ rays in either the forward $(+)$ or backward $(-)$ directions, is then given by integrating over all γ-rays energies x' yielding

$$R_\pm(x)=\frac{2\alpha_\pm C_o f_s t_{\rm ns}}{\pi\rho(1-e^{-t_{\rm ns}})}\int_{-\infty}^{\infty}\frac{1-\exp[-t_s(X)]}{t_s(X)[1+4X^2]}\frac{[r_{c\pm}t\mathcal{L}(2x')+r_{p\pm}t_{\rm na}]}{t\mathcal{L}(2x')+T_\pm}\{1-\exp[-(t\mathcal{L}(2x')+T_\pm)]\}dx'\ . \tag{14}$$

where $R_+(x)$ gives the electrons emitted as a function of x in the forward direction, and $R_-(x)$ gives the same in the backward direction, using the following definitions:

$$T_\pm=t_{\rm na}\mp t_e\ ,$$
$$\alpha_+=\exp[-t_e]\ , \tag{15}$$
$$\alpha_-=1\ .$$

The number of nonresonant γ rays per channel incident on the absorber is given by $(1-f_s)C_o$, and the number of electrons ejected in the forward $(+)$ or backward $(-)$ direction due to these nonresonant photons is given by

$$N_\pm=\frac{(1-f_s)C_o r_{p\pm}t_{\rm na}\alpha_\pm}{T_\pm}\{1-\exp[-T_\pm]\}\ . \tag{16}$$

The total intensity of electrons emitted from the absorbing material out either face is therefore

$$C_\pm(x)=N_\pm+R_\pm(x)\ , \tag{17}$$

where again $C_+(x)$ describes the total number of electrons emitted in the forward position, and $C_-(x)$ describes the total backscattered electrons. Throughout this analysis we neglect background from general sources and downscatter from higher-energy source radioactivity. This is a good description if a monochromating filter is used, as in most of our 46.5-keV tungsten work. Because of the lack of energy discrimination in CEMS and MICE measurements, such a filter is highly desirable to enhance the signal to continuum counts. If this is not done another term is needed to account for this additional background, which is not described by N_+ or N_-. In most CEMS detectors, only $C_-(x)$ is measured and large thicknesses are used such that $t_e\to\infty$. When applied to the MICE detector, this line-shape describes only the first MICE foil, the description for subsequent foils requires modification due to the fact that the γ-ray distribution incident on them has been altered by the resonant and nonresonant absorption that takes place in the preceding foils.

It should be noted that the use of Eq. (12) in the line-shape derivation, where $\sigma_{c\pm}$ is considered proportional to $\sigma_{\rm ra}$, is incorrect. The value of β in $w_s(y)$ and in $\sigma_{\rm ra}$ is that for resonance absorption, and is due to interference between the total nuclear resonance and Rayleigh scattering, and interference between the total internal conversion and photoelectric scattering. The β value calculated in Refs. 5 and 6 corresponds to this absorption interference value. Specifically, the interference parameter for a given multipole transition[10] is $\beta=[\alpha/(1+\alpha)]\beta_c+[1/(1+\alpha)]\beta_R$, where α is the internal conversion coefficient, β_C arises from conversion and photoelectric interference integrated over all angles, and β_R is a similar term arising from interference between Rayleigh and nuclear resonance scattering. The interference value in $\sigma_{c\pm}$ is related to β_C, since it too arises solely from interference

between internal conversion and photolectric scattering, but is averaged only over the forward or backward hemisphere. So while the symmetric part of $\sigma_{c\pm}$ is proportional to $\sigma_{\rm ra}$, the asymmetric (interference) part is not. However, this assumption of equality will generally be good if the Rayleigh contribution to β is negligible, as is often the case, and/or the internal conversion coefficient is such that $\alpha/(1+\alpha)\approx 1$, so that $\beta\approx\beta_C$, and the conversion interference values averaged over the forward and backward hemisphere are approximately equal to each other and hence to β. One can also measure the forward and backward signal simultaneously $[C_+(x)+C_-(x)]$ so that the asymmetry of the two sides are averaged over, decreasing any error due to the difference between the forward and backward conversion interference effects. Although these considerations may cause problems as to the correct physical interpretation of β returned from a least-squares fit, the use of β in such fits will correctly account for the asymmetry in the data, hence ensuring that the other line-shape parameters are not distorted. This is particularly important in measurements of line position v_o, where failure to take line-shape asymmetry into consideration can lead to significant errors in the returned line-position values.

III. ANALYTIC EXPANSION FOR CONVERSION LINE SHAPE

The integral expression for $R_\pm(x)$ can be solved using numerical integration techniques such as Gaussian-Legendre methods. We also give here an analytical expansion based on the Fourier convolution theorem. This method was given in Ref. 7 in detail for the transmission case and here only the results for the conversion case are given. Specifically

$$C_\pm(x)=C_o\alpha_\pm\left\{\frac{(1-f_s)r_{p\pm}t_{\rm na}}{T_\pm}(1-\exp[-T_\pm])+\frac{f_s r_{c\pm}}{\rho}\sum_{k=0}^{\infty}\sum_{m=1}^{\infty}\sum_{j=1}^{m}\tau_k t_{\rm rs}^k t^m A_{j,m}\left[\mathscr{E}_{m-1}-\frac{r_{p\pm}t_{na}\mathscr{E}_m}{r_{c\pm}(m+1)}\right]D_{k,j,m}(x)\right\}, \tag{18}$$

where

$$\mathscr{E}_m=(m+1)\sum_{n=0}^{\infty}\frac{(-T_\pm)^n}{(n+m+1)n!}, \tag{19}$$

$$A_{j,m}=\frac{(-1)^{m+j}2^{j-1}(2m-j-1)!}{4^m m!(m-1)!(m-j)!(j-1)!}. \tag{20}$$

When $T_\pm\to 0$, a condition which often holds when using a single-foil MICE detector, the term in Eq. (18) enclosed in square brackets approaches 1, and the resulting expression for $R_\pm(x)$ has the same functional form and is a mirror image of that found in the transmission case [see Eq. 23)]. The k index in this expansion represents the contribution of SRSA via $t_{\rm rs}$, when SRSA is negligible, $t_{\rm rs}=0$, $\rho=1$, and only $k=0$ contributes to the expansion ($\tau_o=1$), as can be seen directly from Eq. (7) above. The values of $D_{k,j,m}(x)$ must be solved for each k value,[7] the values up to $k=3$ are given in Table I, which we find sufficient for $t_{\rm rs}<1$, as is usually the case. The values of $\mathscr{I}_j(x)$ and $\mathscr{J}_j(x)$ can be found recursively by

$$\mathscr{I}_o(x)=\mathscr{J}_o(x)=0.$$

$$\mathscr{I}_1(x)=\frac{2}{1+x^2},\quad \mathscr{J}_1(x)=\frac{x}{1+x^2}, \tag{21}$$

$$\mathscr{I}_2(x)=\frac{1}{1+x^2}-\frac{2}{(1+x^2)^2},\quad \mathscr{J}_2(x)=-\frac{x}{(1+x^2)^2},$$

and

TABLE I. The $D_{k,j,m}(x)$ terms, where $\mathscr{I}_j=\mathscr{I}_j(x)$, and $\mathscr{J}_j=\mathscr{J}_j(x)$.

k	$D_{k,j,m}(x)$
0	$\mathscr{I}_j-4m\beta\{(j-1)\mathscr{J}_{j-1}+\mathscr{J}_j\}+2m(m-1)\beta^2\{(j-1)(j-2)\mathscr{I}_{j-2}+2(j-1)\mathscr{I}_{j-1}+\mathscr{I}_j\}$
1	$\frac{1}{2}\{\mathscr{J}_j-\mathscr{J}_{j+1}\}+2\beta\mathscr{J}_{j+1}+2m\beta\{(j-1)\mathscr{J}_{j-1}+(2-j)\mathscr{J}_j-\mathscr{J}_{j+1}\}$
2	$\frac{1}{8}\{3\mathscr{I}_j-3\mathscr{I}_{j+1}+\mathscr{I}_{j+2}\}-\beta\{\mathscr{J}_{j+2}-\mathscr{J}_{j+1}\}+\frac{1}{2}m\beta\{3(j-1)\mathscr{J}_{j-1}+3(2-j)\mathscr{J}_j+(j-4)\mathscr{J}_{j+1}+\mathscr{J}_{j+2}\}$
3	$\frac{1}{48}\{15\mathscr{I}_j-15\mathscr{I}_{j+1}+6\mathscr{I}_{j+2}-\mathscr{I}_{j+3}\}-\frac{1}{4}\beta\{3\mathscr{J}_{j+2}-3\mathscr{J}_{j+1}-\mathscr{J}_{j+3}\}+\frac{1}{12}m\beta\{15(j-1)\mathscr{J}_{j-1}+15(2-j)\mathscr{J}_j+(6j-21)\mathscr{J}_{j+1}+(7-j)\mathscr{J}_{j+2}-\mathscr{J}_{j+3}\}$

$$\mathcal{I}_j(x)=\frac{(1-j)}{1+x^2}\left[\left[\frac{j-2}{4}\right]\mathcal{I}_{j-2}(x)+\mathcal{I}_{j-1}(x)\right],$$
$$\mathcal{J}_j(x)=\frac{(1-j)}{1+x^2}\left[\left[\frac{j-2}{4}\right]\mathcal{J}_{j-2}(x)+\mathcal{J}_{j-1}(x)\right]. \quad (22)$$

In general, no more than 25 m terms (and so 25 j terms) are needed in the expansion to give correct results. The experimenter should of course vary these values themselves to ensure sufficient convergence in any particular case.

IV. TRANSMISSION LINE SHAPE

In Mössbauer transmission experiments what is described by the line shape $C(x)$ is the γ-ray intensity that passes through the absorber as a function of the Doppler shifted energy $E_o v/c$. This geometry involves a γ-ray source, a resonant absorber, and a γ-ray detector that measures the γ rays that successfully pass through the detector. The source and absorber are Doppler shifted relative to each other by velocity v. Since resonant absorption is maximum at resonance, the transmission is a minimum at resonance and maximum at off resonance. If the intensity of γ rays per channel incident on the γ-ray detector is given by C_o, then the number of them that are nonresonant is just $f_s C_o$, where again f_s is the effective source fraction of the beam and not the true source recoilless fraction [see Eq. (8)]. The recoilless part is again given by an integral expression, and the complete line shape for transmission, including SRSA, is

$$C(x)=C_o\left\{1-f_s+\frac{2f_s t_{\rm ns}}{\pi\rho(1-e^{-t_{\rm ns}})}\times\int_{-\infty}^{\infty}w_s(X)\exp[-t\mathcal{L}(2x')]dx'\right\}, \quad (23)$$

where $w_s(y)$ is given by Eq. (1). Unlike the conversion line-shape expression, this expression involves no approximations, the absorption of γ rays is clearly known to be exponential and the β value has a clear theoretical interpretation in the transmission case.[5,6] The analytic expansion for this line shape is

$$C(x)=C_o\left\{1-\frac{f_s}{\rho}\sum_{k=0}^{\infty}\sum_{m=1}^{\infty}\sum_{j=1}^{m}\tau_k t_{\rm rs}^k t^m A_{j,m}D_{k,j,m}(x)\right\}. \quad (24)$$

V. HYPERFINE INTERACTIONS AND PARAMETER CORRELATIONS

In this paper we have shown how to express the convolution integral for the line shape for both transmission and conversion-electron ME experiments, and we have given a method for expanding the convolution integral as an analytic convergent series. The results of our analysis are summarized in Eqs. (14) through (20) for the conversion-electron case and Eqs. (23) and (24) for the case of transmission geometry.

Modern high-speed computing techniques have made the need for an analytic expansion more of a source of insight and a reducer of computer time than a necessity. It is possible to vary the line-shape parameters directly within the convolution integral using acceptable times on super and minisuper computers commonly available. A very direct illustration of this direct evaluation of the convolution for a rather complicated case is given in a recent paper by Wagoner, Mullen, and Schupp.[11]

Although the analysis which we have given here is for unsplit and unpolarized ME photon beams, it is possible to generalize the analysis to include hyperfine splittings in the line-shape description.

For an unsplit and unpolarized source with a hyperfine split absorber, configured in transmission geometry, the transmission integral given in Eq. (23) will require modification of the argument of the exponential term inside of the integral. It is at this location that the mathematics must be modified to accommodate the addition of hyperfine interaction physics. For example, suppose that the absorber was polycrystalline and known to have a quadrupole doublet. We would have to modify the generalized Lorentzian term by replacing the single term with two terms. For random orientations in the absence of any asymmetry to the recoilless fraction, we would replace

$$\mathcal{L}(x')\rightarrow\tfrac{1}{2}\mathcal{L}[(2x'+\epsilon)+\mathcal{L}(2x'-\epsilon)], \quad (25)$$

where ϵ is the quadrupole splitting in the dimensions of the level line width.

This modification in Eq. (23) leads to some complications in making an analytic expansion as new cross terms arise. With current computer capabilities the best way to deal with these complications is to vary the line-shape parameters directly within the convolution integral, and avoid the mathematically tiresome process of expanding into an analytic series.

In the above special case, if the two lines were not of equal intensity, either because of a nonrandom distribution of crystallites or due to an anisotropy in f, then the two Lorentzian terms in Eq. (25) could be assigned coefficients c_1 and c_2, whose sum is unity and whose relative values are varied to optimize the agreement between the transmission integral expression (23) and the experimental data. Seeking this additional data, of course, requires adding one additional parameter to the line-shape fitting program.

For magnetically split spectra such as could arise with the 14.4-keV or 46.5-keV ME transitions of ^{57}Fe or ^{183}W, either resolvable or not resolvable six-line hyperfine patterns are expected. This case would require a six-term replacement in the exponential instead of two as shown in Eq. (25). If the direction of the field is known then the coefficients of the six terms can be directly put into the transmission integral. For example, if the B field is in the plane of an ME foil, then the coefficients are in proportion to 3,4,1,1,4,3, with a factor of 16 in the denominator to normalize the coefficients to unity. With a random orientation of fields, only the relative intensity coefficients will change. Unless some constraints on the intrinsic intensities are imposed for these cases the number of pa-

rameters quickly becomes excessive, but this is also true when data are fitted with simple though incorrect Lorentzian functions.

Even in the absence of hyperfine interactions the application of these equations to the fitting of experimental data requires care because of the very high correlation of certain of the line-shape parameters. For example, t_{rs}, t, and Γ all strongly correlate when fitting experimental data, a point that we discussed in detail in an earlier paper.[12] To reduce these correlations it is usually advisable to keep t_{rs} small compared to unity or to carry out an independent measurement to find t_{rs}. The other correlations can be greatly reduced by fitting simultaneously two or more sets of data, taken with absorbers having differing thicknesses, or simultaneously fitting data for several temperatures with known constraints.

In principle, all of the parameters describing an unsplit line, viz., t_{rs}, f_{so}, t, Γ, β, C_o, and v_o, can all be extracted from sufficiently precise data. In some cases even the internal conversion coefficient can be found, as was done for the 46.5-keV line of ^{183}W by Bullard, Mullen, and Schupp[13] (see Sec. 5 of this reference). Since the wavelengths of most ME transitions are well known, this means that the cross section can be found for some cases from the line-shape parameters.

It should be mentioned that the six line-shape parameters used in the fitting of a complicated spectrum can often be fixed from earlier experiments. Thus, the width of the ^{183}W 46.5-keV line is now well known from our earlier work, as well as the interference parameter. Hence, these parameters can be inserted into fits and do not need to be varied as they are invariant for differing materials.

In the conversion-electron measurements the analysis given here requires an additional assumption compared to the transmission case, viz., that the effective likelihood of an internally converted electron registering as a count falls off exponentially with the distance from the surface of the foil to the place where the resonance absorption occurs. This assumption cannot be strictly true, but appears to be a reasonable approximation that leads to a tractable mathematical analysis and result. Careful line-shape studies would be most interesting for conversion-electron detectors and would directly test the exponential falloff assumption used in this analysis.

One interesting result of this analysis that was mentioned in one of our earlier papers[14] is that the conversion-electron ME line is a mirror image of the transmission line only to a first-order approximation. Since there is a passion in the ME field to fit all data to Lorentzian functions, using the width as an experimental parameter, this difference may appear academic, but as we have already noted,[15] the Lorentzian fit to data gives all of the parameters of interest, such as recoilless fraction and interference, seriously in error. These effects are much greater than is generally appreciated by workers in the field.

ACKNOWLEDGMENT

This work was prepared with the support of the U.S. Department of Energy, Grant No. DE-FG02-85 ER 45199.

[1]J. G. Mullen, A. Djedid, C. Holmes, G. Schupp, L. Crow, and W. B. Yelon, Nucl. Instrum. Methods B **14**, 323 (1986).
[2]J. G. Mullen and J. Stevenson, Nucl. Instrum. Methods **153**, 77 (1978).
[3]J. P. Hannon and G. T. Trammell, Phys. Rev. Lett. **21**, 726 (1968).
[4]Yu. Kagan, A. M. Afanas'ev, and V. K. Voitovetskii, Pis'ma Zh. Eksp. Teor. Fiz. **9**, 155 (1969) [JETP Lett. **9**, 91 (1969)].
[5]H. C. Goldwire, Jr., and J. P. Hannon, Phys. Rev. B **16**, 1875 (1977).
[6]B. R. Davis, S. E. Koonin, and P. Vogel, Phys. Rev. C **22**, 1233 (1980).
[7]J. G. Mullen, A. Djedid, G. Schupp, D. Cowan, Y. Cao, M. L. Crow, and W. B. Yelon, Phys. Rev. B **37**, 3226 (1988).
[8]D. Liljequist, J. Phys. D **10**, 1363 (1977).
[9]D. Liljequist and M. Ismail, Phys. Rev. B **31**, 4131 (1985).
[10]V. N. Peregudov, Hyperfine Interact. **3**, 353 (1977).
[11]R. A. Wagoner, J. G. Mullen, and G. Schupp, Phys. Lett. B **279**, 25 (1992).
[12]B. R. Bjullard, J. G. Mullen, and G. Schupp, Hyperfine Interact. **55**, 1127 (1990).
[13]B. R. Bullard, J. G. Mullen, and G. Schupp, Phys. Rev. B **43**, 7405 (1991).
[14]J. G. Mullen, A. Djedid, B. Bullard, G. Schupp, D. Cowan, Y. Cao, and M. L. Crow, Hyperfine Interact. **40**, 123 (1988).
[15]R. A. Wagoner, B. R. Bullard, J. G. Mullen, and G. Schupp, Hyperfine Interact. **77**, 71 (1993).

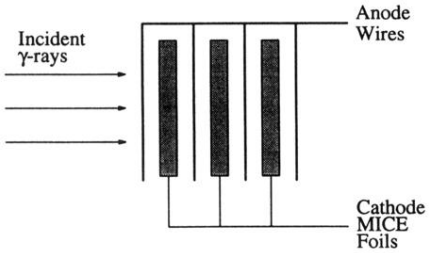

FIG. 1. Geometry of a MICE detector.